EFFECT OF HYDROPHOBIC CHAIN LENGTH ON MELTING TEMPERATURE

ANA FERNANDES, PATRICIA LOSADA-P´EREZ
PHYSIC OF INTERFACES, ULB 2023/2024

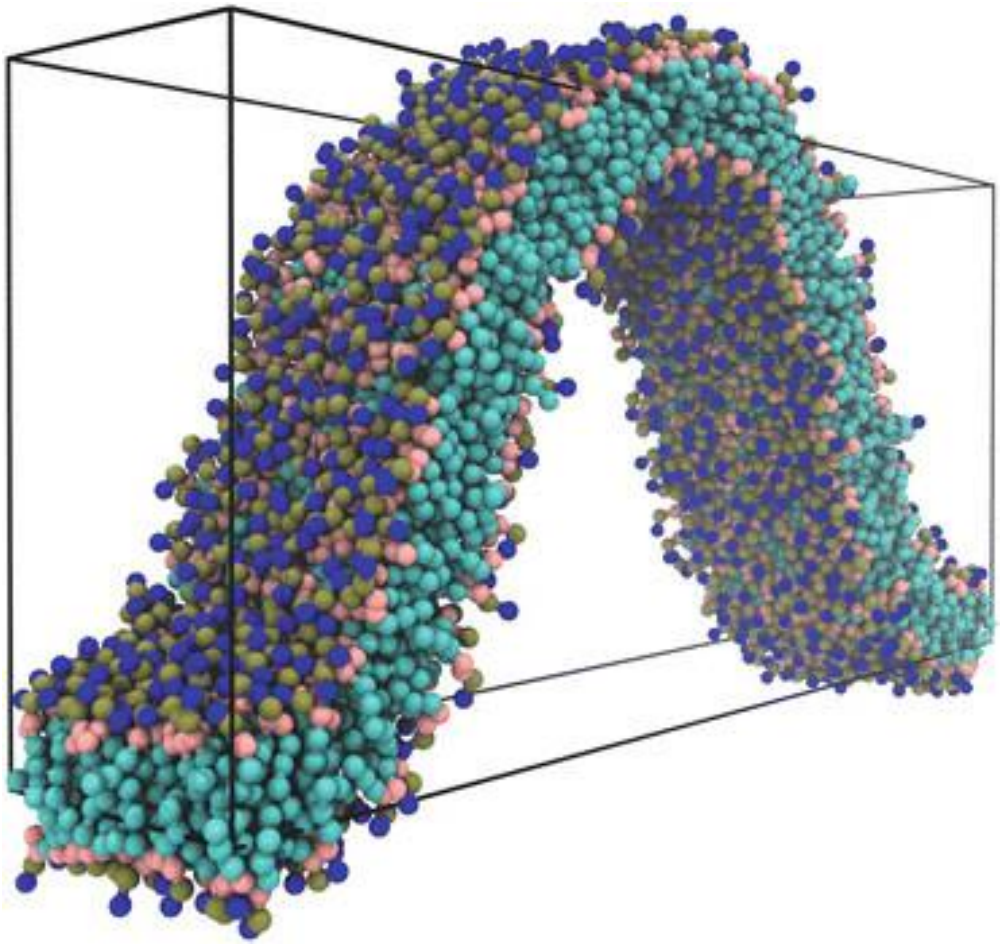

Abstract

Lipid vesicles are model systems for studying cell membranes, they can form intact supported vesicle layers or rupture into lipid bilayers. Information about vesicle properties and behavior is important for studying adhesion, budding, and intercellular communication. In this experiment we will study how vesicle deformation upon adhesion is influenced by lipid organization, using QCM-D as a technique for detecting and characterizing lipid membranes. The paper investigates how the number of carbons in lipid chains affects phase transitions, using DHPC vesicles to characterize phase transition behavior.

1. Introduction

Lipid vesicles are structures that assemble themselves and are commonly employed as model systems for studying the basic properties of cell membranes. When placed on solid surfaces, they can either form intact supported vesicle layers (SVLs) or rupture into planar supported lipid bilayers (SLBs), with a diameter of ≤ 200 nm onto solid surfaces. The geometry of SVLs captures crucial information about the vesicles, including their volume-to-area ratio, adhesion strength, membrane bending properties, and osmotic stress within the supported layer. SVLs are important to study adhesion, budding, lipid membrane exchange, fission, and fusion. SVLs behave like endosomes and exosomes assuming chemical transport and intercellular communication. [7]

Through the study of the adhesion, bending, and geometrical constraints, we can determine the vesicle's shape upon adsorption.

$$F = \frac{1}{2}k\oint (C1 + C2 - C0)^2 dA + kG\oint C1C2dA - WAc + PV + \sum A$$

The free energy expression F for an adsorbed vesicle considers adhesion energy, local bending energy, and geometrical constraints. The terms in the equation involve the local bending modulus (κ), Gaussian curvature modulus (κ G), principal curvatures (C1, C2), effective spontaneous curvature (C0), and other parameters.

Vesicle deformation upon adhesion is strongly influenced by the lipid organization of the vesicle membrane, which is connected to its phase behavior. Traditional calorimetric approaches are often hindered by the optical inaccessibility of vesicles with diameters ≤ 200 nm and the instability of small unilamellar vesicle (SUV) dispersions.

In this context, the quartz crystal microbalance with dissipation monitoring (QCM-D) has emerged as a versatile technique for detecting and characterizing phase transformations in solid-supported lipid membranes. QCM-D, an acoustic-based, label-free technique, is highly sensitive to changes in mass and energy dissipation at the solid-lipid layer-liquid interface. It has proven useful in studying kinetics, adsorption, and formation of supported lipid bilayers, as well as probing their interactions with biomolecules.[4]

In this experience we used QCM-D to investigate how the number of carbons in the lipid chain influences phase transitions in solid-supported membranes. Diheptadecanoylphosphatidylcholine (DHPC) vesicles were chosen to characterize phase transition behavior. For that we used a solid surface of polycrystalline Au and the theorical values for the adhesion level of SiO2. The correlation between surface wettability and membrane phase transitions is explored in relation to vesicle size and adsorption temperature.

2. Materials and methods

2.1. Materials

DHPC has two heptadecanoic acid (17-carbon) chains attached to the glycerol backbone, and it is a phosphatidylcholine like DPPC but with longer acyl chains. A pH 7.4 HEPES buffer was prepared, consisting of 10 mM HEPES (99%) and 150 mM NaCl, both sourced from Sigma-Aldrich (≥99.5%). This buffer solution was utilized to rehydrate the dried lipid films. The lipid quantities were determined through gravimetric analysis, employing an analytical balance. [7]

2.2. Vesicle preparation

The DHPC lipid in powder form was initially dissolved in spectroscopic grade chloroform, and the solvent was evaporated under a gentle flow of nitrogen in a round-bottomed flask. Subsequently, the lipid film underwent low-pressure conditions overnight to eliminate any remaining solvent traces. All the process until this part was developed by the professor on the day before the experiment. The film was then hydrated with HEPES buffer to achieve a concentration of 1 mg/mL under continuous stirring in a temperature-controlled water bath at 55 °C, a little bit above the melting temperature of DHPC (Tm ~ 50°C).

Following, 10,5 mg of lipid was suspended in 3.5 mL of HEPES, obtaining a final concentration of 3mg/mL. And

4mg of lipid was suspended in 2mL of HEPES, obtaining a final concentration of 2mg/mL. After that, 1ml of the solution was extruded using a membrane with 100nm diameter, passing 22 times, forming LUVs.. After extruded we obtained a final concentration of 0.5mg/mL.

2.3. Quartz crystal microbalance with dissipation monitoring (QCM-D)

The study employed a Qsense E4 instrument (Gothenburg, Sweden) to monitor frequency and dissipation changes (Δf and ΔD). The Q-sense E4 apparatus allowed for temperature scans in the range of 15 °C to 65 °C. AT-cut quartz crystals with Au coating (diameter 14 mm, thickness 0.3 mm, quoted surface roughness < 3 nm, and resonant frequency 4.95 MHz) were utilized. [5]

Initially, a baseline was established with pure HEPES buffer, followed by the injection of lipid vesicles over the Au-coated sensor chips. Once a stable supported membrane layer was achieved, the pump was switched off, and the ensemble was left to stabilize for several hours. Subsequent temperature scans, involving both heating and cooling, were performed at a rate of 0.4 °C/min, with a 60-minute stabilization time between successive temperature ramps. The measurements were repeated at least three times to assess the reproducibility of the results.[4]

2.4. UV-Ozone

During the surface preparation the Au-coated quartz sensors were cleaned by immersions for 5 min in a 5:1:1 mixture of milli-Q water, ammonia and hydrogen peroxide heated at 75°, subsequently rinsed in milli-Q water and dried with N2. Shortly prior to the beginning of the QCM-D measurements, Au sensors were exposed to UV-light for 15 min using a UV-ozone cleaner (Bioforce Nanosciences, Wetzlar, Germany).

UV-Ozone cleaning is generally effective for removing organic contaminants [6]. Organic compounds are converted into volatile substances (e.g., water, carbon dioxide, nitrogen) by decomposition by ultraviolet rays and by strong oxidation during the formation and decomposition of O_3 and are removed from the contaminated surface. The major wavelengths of the ultraviolet rays radiated from a well-known low-pressure mercury vapor lamp are 184.9 nm and 253.7 nm. When atmospheric oxygen O_2 is irradiated with ultraviolet rays with a wavelength of 184.9 nm, the oxygen absorbs the ultraviolet rays to form O_3 by the following reaction:

$$O_2^- > O + O$$

$$O + O_2^- > O_3$$

Ozone O_3 irradiated with ultraviolet rays with a wavelength of 253.7 nm absorbs the ultraviolet light to decompose O_3. During the process of formation or decomposition of O_3, atomic oxygen O having a strong oxidizing ability is generated. Then, contaminant organic compounds are irradiated with ultraviolet rays, and absorb the ultraviolet rays to cause photolysis and generate the following substances: Ions, Free radicals, Excited molecules, Neutral molecules, etc.

2.5. Contact angle and surface energy

Contact angle (CA) measurements were conducted employing an Attension ThetaLite apparatus from Biolin Scientific (Sweden), utilizing the sessile drop method. A minute drop (3 μ L) of either Milli-Q water or was placed onto meticulously cleaned, UV-ozone treated Au-coated. The contact angle of the 3 μ L droplet was ascertained by doing the average of several drops over a 10-second period using a recording speed of 20 frames per second. Contact angles were measured at various points, and an average value was derived. All contact angle measurements were conducted at room temperature. Surface free energies of UV-ozoned Au surface (including polar γ svp and dispersive γ svd components) was determined based on the obtained contact angle data.

Sample	$\theta(°)_{water}$	$\theta(°)_{DI}$	γ_{sv}	γ^{d}_{sv}	γ^{P}_{sv}	W_{sl}
Au	34,8±0,21	20,0±0,20	60,36 ±0,39	47,77	12,59	132,58± 0,33

Tabel 1- Surface Energy

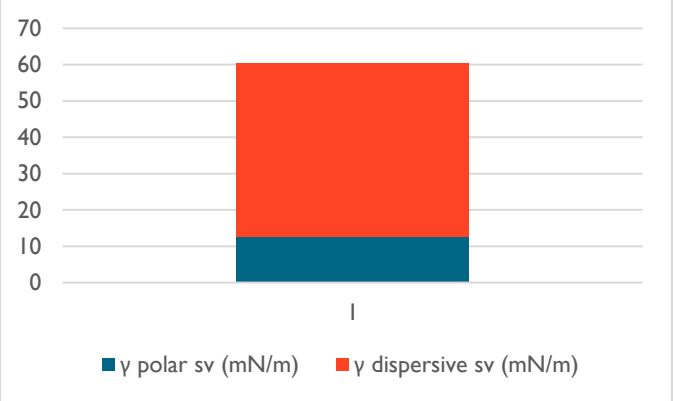

Figure 1- Dispersive and polar components in Au

3. Results and discussion

3.1. Lipid adsorption and layer formation

To understand the adsorption process and layer formation, we plot the variation in frequency (Figure 2) and dissipation (Figure 3) depending on the time of experiment.

Adsorption refers to the accumulation of molecules or particles at a surface. In our experiment, the solid surface is the quartz crystal in the QCM-D instrument, and the liquid phase contains the lipid vesicles.

Initially, the lipid vesicles adsorb onto the QCM-D surface. The vesicles might interact with the surface through electrostatic forces, Van der Waals forces. During this first adsorption (1), the frequency reaches a lower constant plateau, and the dissipation a higher constant plateau, they're called non-zero plateau.

To analyze the lipid behavior during this phase, we plotted two graphics, the first one (figure 4) corresponding to the frequency, and the second one (figure 5) corresponds to the dissipation variance when the temperature was 16°C.

Note: My relevant data starts on the 812th second, so the beginning of the graph in on x = 800.

At T<Tm, 16°C, the lipid bilayer has a vesicle form, as it shown on figure 4, which means that it's in the gel phase. At this phase, the bending modulus kc is larger, and the lipid vesicle is stronger. This can result in a relatively high frequency shift on the QCM-D. The rigid and ordered structure of the vesicles would result in less energy dissipation during the crystal oscillation, as we can see in the 2nd zone in figure 2 and 3.

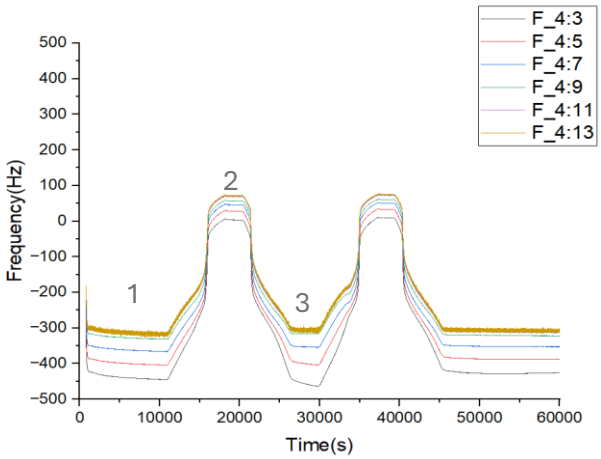

Figure 2- Frequency depending on time.

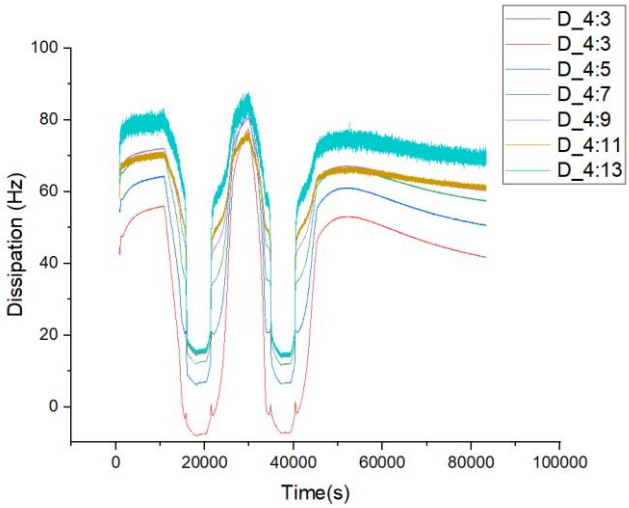

Figure 3 – Dissipation depending on time.

Lipid molecules in a vesicle have hydrophobic tails and hydrophilic heads. The transition from a rigid state to a fluid state is often associated with the melting of lipid chains. In a rigid state, the lipid chains are ordered and tightly packed, creating a more solid-like structure. As we heated the solution, the kinetic energy of the molecules increases, because the thermal energy supplied to the system overcomes the energy barriers that maintain the ordered state of the lipid chains, leading to the disruption of these ordered structures. Near the melting point, lipid chains start to lose their ordered structure increasing lateral mobility. This increases fluidity on the adsorbed layer, making it more dynamic and possibly less tightly packed. Resulting to a lipid bilayer

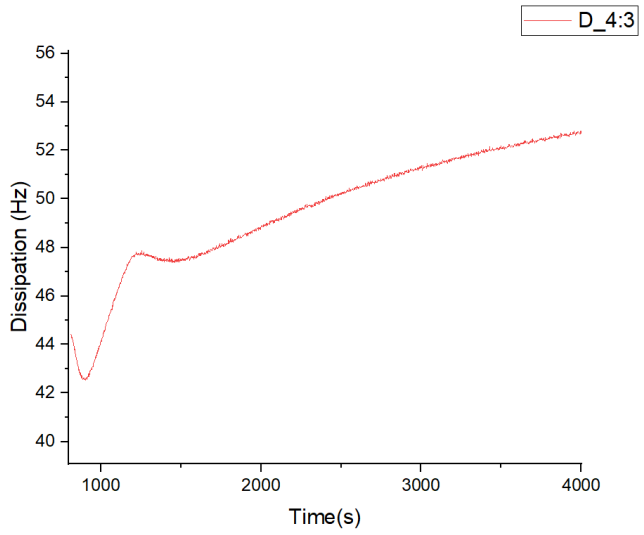

Figure 5 – Dissipation of the 1st overtone depending on time at 16°C

transitions from a gel-like, rigid state to a more disordered, fluid state, with a bending module K much smaller.

This happens on stage 3 marked on figure 2 and 3, when T>Tm, the frequency reaches a minimum value and the dissipation a maximum one. This results from a reduction in the mass density on the QCM surface, resulting in a decrease in frequency variance. The more

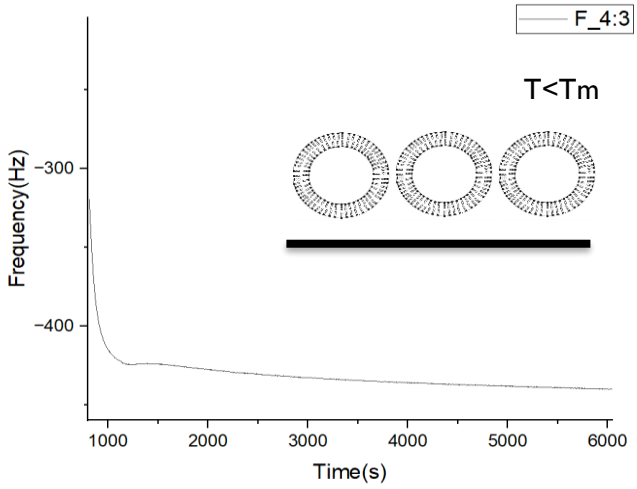

Figure 4 – Frequency depending on time of the 1st overtone (4:3) at 16°C.

fluid and dynamic nature of the bilayer contributes to greater dissipation.

The lipid phase behavior can be related to vesicle dispersions that were evaluated by density measurements (figure 6). To do this relation it was calculated the specific volume of the lipid V_L using the following equation:

$$VL = \frac{VS - (1 - WL)\, v\,(buffer)}{WL}$$

Where $V_S = 1/\rho_S$, is the lipid plus HEPES volume, $v_{buffer} = 1/\rho_{buffer}$, the HEPES volume, with ρ_s the lipid plus HEPES density and p the buffer (HEPES) density. The lipid's specific volume has changed at approximately 50°, which indicates the phase transition moment, where the lipid bilayer acquired a fluid behavior. The lipid volume Vs increase as the density decrease according to figure 6.

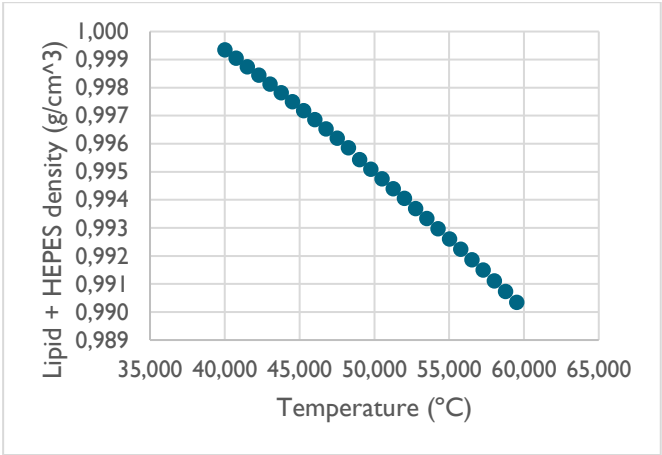

Figure 6- Density change in order of temperature.

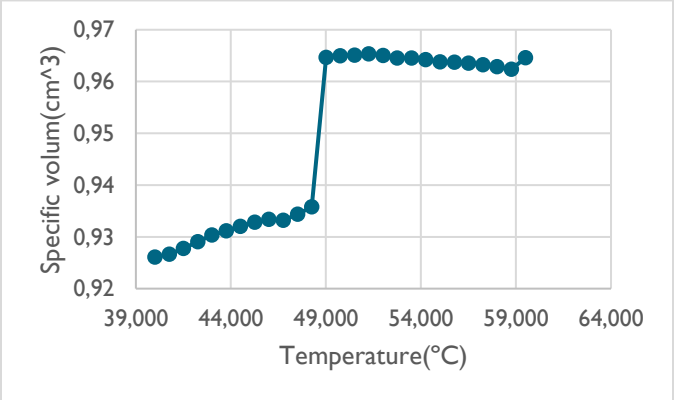

Figure 7- Phase transition

3.2. Vesicle thickness

With the QMC-D information we can estimate the extent of vesicle deformation upon adsorption following a model-free approach introduced by Tellechea *et al.*(Tellechea et al., 2009) [1]. This method consists in plotting –ΔD/Δf ratio vs –Δf for all overtones during initial adsorption, which shows a linear decrease over a large range of frequency shifts (figure 8). Extrapolation of this linear decrease to a frequency-independent intercept with the –Δf axis (where overtones intersect) provides a value of the thickness of the adsorbed vesicle layer h or Sauerbrey thickness:

$$h = -\Delta f \, . \, C/\rho$$

With C = 18ng/cm² and ρ = 1g/cm³.

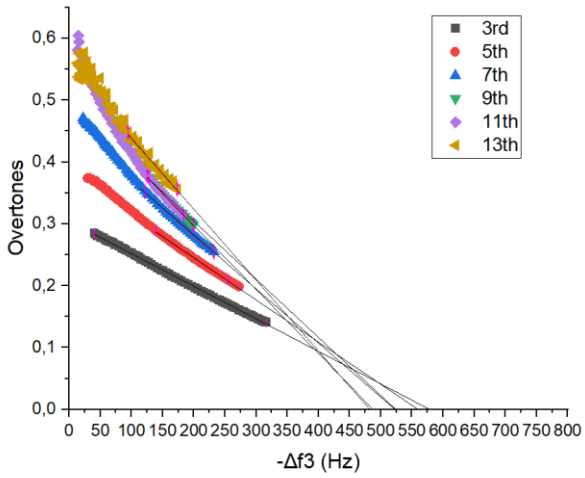

Figure 8 – (- Δf)/ (ΔD) depending on (- Δf) for 5 overtones.

Overtone	-Δf(Hz)	h(nm)
3rd	577,1583	103,8885
5th	556,8505	100,2331
7th	516,4302	92,9574
9th	476,3925	85,7507
11th	476,6729	85,8011
13th	480,3826	86,4689

Table 2 – (-Δf) and Sauerbrey thickness for corresponding overtone at 16°C

The membrane we used had a diameter of 100nm, because of that we extruded vesicles with 100nm. The vesicle thickness that we observed after lipid adsorption, by using Sauerbrey equation and the technique of extrapolation mentioned previously, is mentioned in the following table, and the corresponding comparison with the initial thickness.

	h(nm)	Δd(%)
LUVs in Au	92,52 ± 9,06	7,49±5,19

Table 3- Sauerbrey thickness and corresponding extent of vesicles deformation.

3.3. Temperature influence in phase transition

To better understand the transition phase, we can analyze how the frequency changes with the temperature. When the temperature reaches 50°C it's clear the quick change in the frequency, which indicates that the lipids are changing phases, acquiring a fluid behavior (figure 9). By making a derivative curve of the Δf3/T (figure 10) we obtained a single peak anomaly that takes place at the temperature when the DHPC has it melting point, as expected. We can also see at 40°C a small peak, that's more visible when it's applied a smoothing filter on the derivate, this small peak indicates a pre-transition moment. [3]

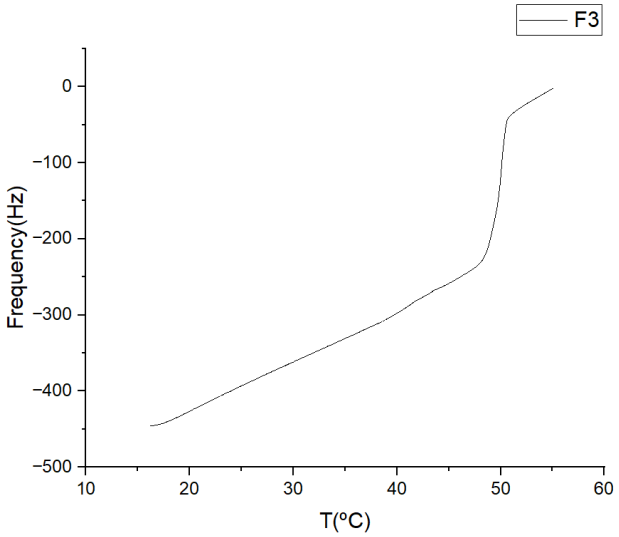

Figure 9- Frequency change in order of temperature

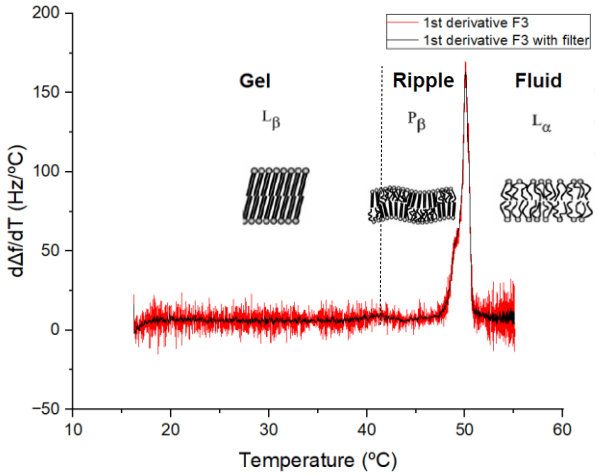

Figure 10 – Derivative of frequency change in order of temperature

3.4. Comparison of melting points

In this experiment we calculate the importance of the chain length on melting temperature for DIPC (15:0C) and DHPC (17:0C).

It's noticeable by observing figures 11 and 12 that the melting point for the lipid with 15 carbons has a lower temperature than the 17 carbons lipid. The reason is because the second lipid has a longer chain length, with more carbon atoms. The observed phenomenon will be better explained in the conclusion.

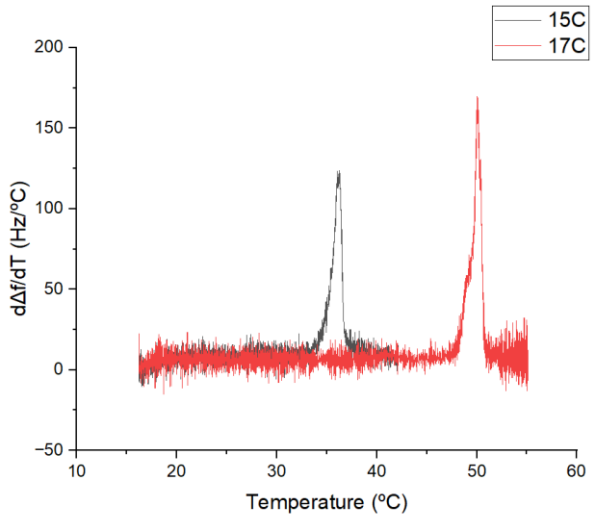

Figure 11- Transition peaks for 15:0 and 17:0 lipids

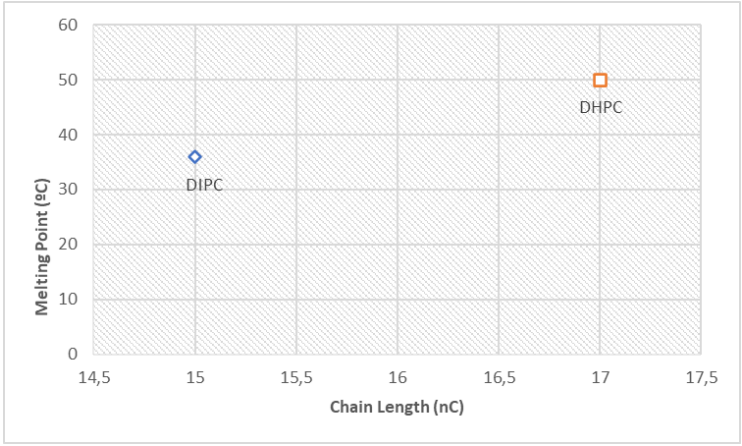

Figure 12- Melting point for 15:0 and 17:0 lipids

4. Conclusion

We made this experiment to study the adhesion and phase behavior of different lipids in Au surface to understand how the chain length influences the melting point of the lipid. The derivative dΔf/dT show the temperature where the phase transition occurs, and it's a clear indicative of how this temperature changes depending on the number of carbons in the lipid chain. This phenomenon is justified by the fact that longer lipid chains generally have stronger van der Waals forces between molecules. As chain length increases, more energy is required to break these forces during the melting process. The enthalpy change (ΔH) for melting longer-chain lipids is typically higher than for shorter-chain lipids [8]. The entropy (ΔS) is also higher for long chain lipids, however, the enthalpy changes are more significant in the Gibbs free energy, $\Delta G = \Delta H - T\Delta S$, which indicates that long-chain lipids have higher melting temperatures and short-chain lipids have lower melting temperatures.

References

1. L. Redondo-Morata, P. Losada-Pérez & M. I. Giannotti- Lipid bilayers: phase behavior and I nanomechanics
2. Laure Bar, Martín Eduardo Villanueva, Claudio Martín, Andrea Valencia Ramirez, Jonathan Goole, Frank Uwe Renner, Patricia Losada-P´erez - Stability of supported hybrid lipid bilayers on chemically and topographically-modified surfaces
3. T. N. Murugova and P. Balgavy - Molecular volumes of DOPC and DOPS in mixed bilayers of multilamellar vesicles
4. Shova Neupane, Yana De Smet 1, Frank U. Renner and Patricia Losada-Pérez - Quartz Crystal Microbalance With Dissipation Monitoring: A Versatile Tool to Monitor Phase Transitions in Biomimetic Membranes
5. Derick Yongabi, Mehran Khorshid, Alessia Gennaro, Stijn Jooken, Sam Duwé, Olivier Deschaume, Patricia Losada-Pérez, Peter Dedecker, Carmen Bartic, Michael Wübbenhorst, and Patrick Wagner, QCM-D Study of Time-Resolved Cell Adhesion and Detachment: Effect of Surface Free Energy on Eukaryotes and Prokaryotes
6. JOHN R. VIG: IEEE TRANSACTIONS ON PARTS, HYBRIDS, AND PACKAGING, VOL. PHP-12, NO. 4, DECEMBER 1976
7. N. Bibissidis, K. Betlem, G. Cordoyiannis, F. Prista-von Bonhorst, J. Goole, J. Raval, M. Daniel, W. Góźdź, A. Iglič, P. Losada-Pérez, Correlation between adhesion strength and phase behaviour in solid-supported lipid membranes.
8. Thomas Heimburg, Thermal Biophysics of Membranes.